Electromagnetic Characterization of Textured Surfaces Formed by Metallic Pins

Mário G. Silveirinha, *Member, IEEE*, Carlos A. Fernandes, *Member, IEEE*, and Jorge R. Costa, *Member, IEEE*

***Abstract*—We develop a homogenization model to characterize textured surfaces formed by a periodic arrangement of thin metallic pins attached to a conducting ground plane: the "Fakir's bed of nails" substrate. It is demonstrated that the textured surface can be accurately modeled using a dielectric function, provided spatial dispersion effects are considered as well as additional boundary conditions. We derive closed analytical formulas for the reflection coefficient, and for the dispersion characteristic of the surfaces waves. In addition, it is demonstrated that the artificial substrate may mimic almost exactly the behavior of an ideal impedance surface boundary, and that the only physical factor that may limit this remarkable property is the skin depth of the metal. The reported results are supported by full wave simulations as well as by experimental data.**

***Index Terms*—Additional boundary conditions (ABC), high impedance surfaces, metamaterials, surface impedance, wire media.**

I. Introduction

THE possibility of designing microstructured materials that interact with electromagnetic waves in a controlled and desired way opens new research avenues that may enable the realization of novel compact resonators, and waveguides that may overcome diffraction limits [1]–[4], which were thought insurmountable. Some interesting and promising opportunities include the realization of imaging devices with super-resolution [5]–[7], or the transmission of waves through very narrow channels with great electric field enhancement [8].

The design of compact textured surfaces with desired characteristics, (e.g. realization of surface impedances or tailoring the properties of surface waves), is also an important and mature field of research [9]–[12]. Recently, it was suggested that by corrugating the surface of a metallic wire it may be possible to excite highly localized modes which may open the way for applications such as energy concentration and superfocusing using conical structures at terahertz or microwaves [13]. Another stimulating field of research at microwaves is the realization of artificial ground planes that may enhance the radiation properties of low-profile antennas [14]–[24]. Textured surfaces may be used to change the surface impedance, control the reflection characteristic, and tailor the propagation properties of surfaces waves. In [15] it was demonstrated that a properly designed textured surface formed by mushroom-shaped metal implants may behave as a compact high-impedance boundary, and may inhibit the propagation of surface waves for both polarizations. This type of artificial substrates may have important applications in wireless communications because they are lightweight, low cost, and very compact, being a good solution for the design low profile antennas with a good return loss over a relatively wide bandwidth, or to eliminate the mutual coupling in a microstrip antenna array sharing the same ground plane, just to mention a few possibilities [14]–[24].

The objective of this work is to study the properties of textured surfaces formed by metallic pins embedded in a dielectric substrate and attached to a conducting plane, in a topology resembling a "Fakir's bed of pins." Even though some of the basic properties of such artificial surface have been known for some time [25], and have been revisited recently [24, p. 231], [26], we believe that some important points remain unaddressed or are not completely well understood. In fact, in previous works the Fakir's bed substrate was identified with a wire medium slab following a local permittivity model [25], [26], and the spatial dispersion effects were neglected. However, it has been recently demonstrated [27]–[29] that wire media formed by continuous wires are strongly spatially dispersive, and thus it may be necessary to take into account the non-locality of these media to properly describe the interaction of electromagnetic waves with the artificial substrate under study. In this work, we derive a new homogenization model for the "Fakir's bed substrate" that takes into account these nonlocal effects and provides a correction to the results reported in [25]. It is shown that the new model can predict accurately the reflection of plane and evanescent waves, as well as the dispersion characteristic of surface waves. We study the conditions that are necessary to suppress the propagation of surfaces waves in the artificial substrate, and investigate when the textured surface can be characterized by an equivalent surface reactance. Our theoretical model suggests that provided losses are negligible and one is able to fabricate very dense arrays of metallic wires, there is no physical limit on how well the Fakir's bed substrate may mimic the behavior of a desired surface reactance. Moreover, the effect of metallic losses is also investigated and it is shown that the performance of the artificial impedance boundary is only limited by the skin depth of the

Manuscript received February 26, 2007; revised July 23, 2007. This work was supported by the Fundação para Ciência e a Tecnologia under project POSC/EEACPS/61887/2004.

M. G. Silveirinha is with the Electrical Engineering Department, Instituto de Telecomunicações, Pólo II da Universidade de Coimbra, 3030 Coimbra, Portugal (e-mail: mario.silveirinha@co.it.pt).

C. A. Fernandes is with Instituto de Telecomunicações-Instituto Superior Técnico, 1049-001 Lisboa, Portugal.

J. R. Costa is with Instituto de Telecomunicações-Instituto Superior Técnico, 1049-001 Lisboa, Portugal and also with the Instituto Superior de Ciências do Trabalho e da Empresa, 1649-026 Lisboa, Portugal.

Color versions of one or more of the figures in this paper are available online at http://ieeexplore.ieee.org.

Digital Object Identifier 10.1109/TAP.2007.915442

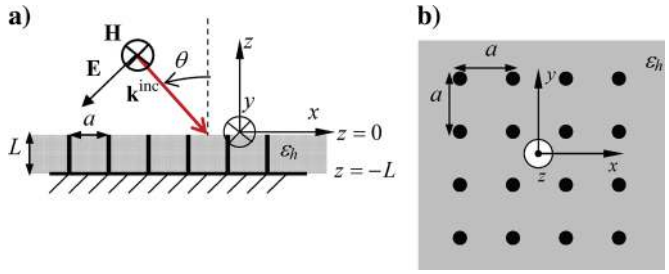

Fig. 1. Geometry of the "Fakir's bed of nails" substrate (Panel (a): side view; Panel (b): top view). The textured surface is formed by a square lattice of metallic pins, embedded in a dielectric substrate with permittivity ε_h and height L. The pins are connected to the PEC ground plane and the spacing between the pins is a.

metal pins. The pr[illegible]ted theory is validated using numerical simulations, and in addition with experimental results obtained for a closed metallic waveguide configuration in which one of the waveguide walls is the textured surface under study.

This paper is organized as follows. In Section II, we examine the reflection properties of the Fakir's bed of nails substrate and the propagation of surface w[illegible]. We study in which conditions the artificial substrate may, in fact, be approximated by an equivalent impedance boundary. In Section III, the effect of metal losses is examined and a simple criterion to assess its relative importance is proposed. In Section IV, we report experimental results that validate our theory in a realistic setup. Finally, in Section V the conclusions are drawn.

II. Homogenization of the Textured Surface

The geometry of the textured substrate under study is depicted in Fig. 1. It consists of a square array of cylindrical metallic pins with radius r_w, embedded in a dielectric substrate with (relative) permittivity $\varepsilon_h$and height L. The spacing between the pins (lattice constant) is a. Note that the metallic pins are connected to a perfect electric conductor (PEC) ground plane.

As discussed in [25], the "Fakir's bed of nails" may be used to synthesize an artificial impedance reactance. A recent study about the characterization and design of impedance boundaries can be found in [30]. It is well known that metallic pins (vias) allow for the suppression of surface waves in the Sievenpiper mushroom structure [15], [23], [26]. It is also interesting to note that the mushroom surface proposed in [15], can be regarded as a "Fakir's bed" substrate in which the corrugations have been folded up into lumped-circuit elements, in order to save space along the z-direction and obtain a low-profile characteristic.

Next we propose an approximate analytical method to characterize the Fakir's bed of nails using homogenization theory.

A. Reflection Characteristic

The objective is to calculate the reflection coefficient when the textured surface is illuminated by an incoming plane wave with wave vector $\mathbf{k}^{\text{inc}}$, as illustrated in Fig. 1. In order to obtain an analytical model that may simplify an otherwise very complex problem, we will regard the array of metallic pins as a truncated wire medium. [illegible] in [25], [26] a similar approximation was used, however the novelty of our treatment is that it fully considers and takes into account the effects of spatial dispersion using the ideas proposed in our previous work [31]. Spatial dispersion is intrinsic to artificial media formed by long metallic inclusions [27], [28]. Next, the basic properties of wire media are briefly reviewed.

Following [27], the wire medium is a microstructured material formed by infinitely long thin metallic rods. For long wavelengths it may be characterized by the dielectric function

$$\begin{aligned}\overline{\overline{\varepsilon}}_{\text{eff}} &= \varepsilon_0\varepsilon_h\left(\hat{\mathbf{u}}_x\hat{\mathbf{u}}_x + \hat{\mathbf{u}}_y\hat{\mathbf{u}}_y + \varepsilon_{zz}(\omega,k_z)\hat{\mathbf{u}}_z\hat{\mathbf{u}}_z\right)\\ \varepsilon_{zz}(\omega,k_z) &= 1 - \frac{\beta_p^2}{\beta_h^2 - k_z^2}\end{aligned} \tag{1}$$

where ε_h is the relative permittivity of the host material, $\beta_h = \beta\sqrt{\varepsilon_h}$ is the wave number in the host material, $\beta = \omega/c$ is the wave number in free-space, k_z is the z-component of the wave vector $\mathbf{k} = (k_x, k_y, k_z)$ of a plane wave, and β_p is the plasma wave number, which only the depends on the geometrical properties of the lattice [27]

$$(\beta_p a)^2 = \frac{2\pi}{\ln\left(\frac{a}{2\pi r_w}\right) + 0.5275}. \tag{2}$$

The homogenization model predicts that the wire medium supports three different families of plane wave solutions: transverse electromagnetic (TEM) modes, transverse magnetic (TM-z) modes, and transverse electric (TE-z) modes. The dispersion characteristic of these modes is

$$\beta_h = \pm k_z \quad (\text{TEM mode}) \tag{3a}$$
$$\beta_h^2 = k^2 \quad (\text{TE mode}) \tag{3b}$$
$$\beta_h^2 = \beta_p^2 + k^2 \quad (\text{TM mode}) \tag{3c}$$

where $k^2 = \mathbf{k}.\mathbf{k}$.

Consider that a plane wave illuminates a wire medium slab (the textured surface), as depicted in Fig. 1. The wave vector of the incoming wave can be written as $\mathbf{k}^{\text{inc}} = \mathbf{k}_{\|} - j\gamma_0\hat{\mathbf{u}}_z$, where $\mathbf{k}_{\|} = (k_x, k_y, 0)$ is the component of the wave vector parallel to the interface (for a propagating wave $k_{\|} = \beta\sin\theta$, where $\beta = \omega/c$ and θ is the angle of incidence), and $\gamma_0 = \sqrt{k_{\|}^2 - \beta^2}$. When the polarization of the incoming wave is TE, with electric field parallel to the ground plane, it does not interact with the metallic wires and thus, for TE polarization, the textured substrate is equivalent to a dielectric slab backed by a PEC plane.

Consider now that the incoming wave is TM-polarized, with magnetic field horizontal with respect to the ground plane (see Fig. 1). For this polarization, the incident wave can induce an electric current along the metallic pins, and thus excite the TEM and TM modes in the wire medium slab (the TE-mode is not excited). It is assumed without loss of generality that the incoming wave has normalized amplitude with magnetic field along the y-direction, $\mathbf{H}^{\text{inc}} = e^{+\gamma_0 z}e^{-jk_x x}\hat{\mathbf{u}}_y$, but the final formulas presented below are valid in the general case. Since the transverse component $\mathbf{k}_{\|}$ of the wave vector is preserved, the magnetic field in all space can be written as [31]

$$H_y = (e^{+\gamma_0 z} + \rho e^{-\gamma_0 z})e^{-jk_x x} \quad (\text{air side} : z > 0) \tag{4a}$$
$$= \left(B_{\text{TEM}}^{+}e^{-j\beta_h z} + B_{\text{TEM}}^{-}e^{+j\beta_h z}\right.$$

$$+B^{+}_{\mathrm{TM}}e^{-\gamma_{\mathrm{TM}}z}+B^{-}_{\mathrm{TM}}e^{+\gamma_{\mathrm{TM}}z}\big)\,e^{-jk_x x}$$
$$(\text{wire medium slab}: -L<z<0) \tag{4b}$$

where $\gamma_{\mathrm{TM}}=\sqrt{\beta_p^2+k_\parallel^2-\beta_h^2}$ is the propagation (attenuation) constant along the z-direction of the TM mode, ρ is the reflection coefficient, and $B^{\pm}_{\mathrm{TEM}}$ and $B^{\pm}_{\mathrm{TM}}$ are the amplitudes of the excited TEM and TM waves, respectively. To determine the unknown coefficients it is necessary to impose boundary conditions at the interfaces $z=0$ and $z=-L$. The classic boundary conditions impose that the tangential electric and magnetic fields are continuous at $z=0$ (interface with air), and that the tangential electric field vanishes at $z=-L$ (interface with PEC plane). However, it is easy to verify that such boundary conditions are insufficient to calculate the unknown coefficients. In fact, there are five unknowns, ($B^{\pm}_{\mathrm{TEM}}$ and $B^{\pm}_{\mathrm{TM}}$ and ρ), and only three independent equations. Indeed, as discussed in [31] the classical boundary conditions are insufficient to solve scattering problems in wire media (or more generally in spatially dispersive media [32]). To circumvent this difficulty, in [31] we introduced an *additional boundary condition* (ABC) that removes the extra degrees of freedom. We demonstrated that at an interface between the wire medium and air we have

$$\varepsilon_h\mathbf{E}.\hat{\boldsymbol{\nu}}|_{\text{wire medium side}}=\mathbf{E}.\hat{\boldsymbol{\nu}}|_{\text{air side}} \tag{5}$$

where $\hat{\boldsymbol{\nu}}$ is the normal to the interface ($\hat{\boldsymbol{\nu}}=\hat{\mathbf{u}}_z$ in Fig. 1). Note that the above condition is not equivalent to the continuity of the electric displacement vector, since the effective permittivity of the wire medium is not ε_h. This new boundary condition was successfully validated in the study of the imaging properties of wire medium slabs at microwaves [33], terahertz, and infrared frequencies [7]. As mentioned in [31], the continuity of H_y, the continuity of the tangential electric field E_x, and the ABC (5), are ensured by the conditions

$$[H_y]=0;\quad \left[\frac{1}{\varepsilon_h(z)}\frac{dH_y}{dz}\right]=0$$
$$\left[\frac{d^2H_y}{dz^2}\right]=\left(\beta_h^2-\beta^2\right)H_y \tag{6}$$

respectively, where $[\ldots]$ represents the jump discontinuity of the function inside rectangular brackets at the interface, i.e., the function evaluated at the air side minus the function evaluated at the wire medium side. We define $\varepsilon_h(z)$ in such a way that $\varepsilon_h(z)=1$ at the air side, and $\varepsilon_h(z)=\varepsilon_h$ (permittivity of the substrate) at the wire medium side.

Imposing the ABC at the interface between the wire medium and air, we remove one degree of freedom of the scattering problem. However, the problem is still underdetermined because there are five unknowns and only four equations (three equations at the interface with air, as suggested by (6), and a single equation, $(1/\varepsilon_h)(dH_y/dz)=0$, at the PEC interface, $z=-L$, which is equivalent to impose that the tangential electric field vanishes at the PEC plane). In fact, to obtain a definite system we also need to impose an ABC at the interface between the PEC ground plane and the wire medium. However, the ABC given by (5), cannot be applied at $z=-L$. In fact, (5) was derived in [31] based on the hypothesis that the current that flows along the thin metallic pins is approximately zero at the pertinent interface. This is certainly true when the material adjacent to the wire medium slab is non-conductive (e.g., a regular dielectric). However, if the pins are connected to a PEC ground plane (as in Fig. 1), it is obvious that the current along the pins may be non trivial at the interface, and thus (5) is not applicable in such conditions.

Even though it is possible to formulate a general ABC appropriate to characterize the electromagnetic fields at an interface between a wire medium slab and a PEC ground plane (this will be discussed in a future publication), next we will follow a simpler and more direct approach to solve the scattering problem. In fact, it is enough to notice that because of the symmetry of the Fakir's bed substrate, the tangential electric fields associated with the TE, TM, and TEM electromagnetic modes must vanish independently at the PEC ground plane. The situation is somehow analogous to what happens in a 3D rectangular metallic waveguide terminated by a standard short-circuit (PEC wall). Indeed, also in such case when a wave impinges on the short-circuit load, the tangential electric field associated with each waveguide mode vanishes independently at the PEC wall. This happens because the transverse electric field distributions of the waveguide modes are orthogonal at the PEC wall. Similarly, it can be proved that for the Fakir's bed substrate depicted in Fig. 1 (with vertical pins), the electric field distributions of the (non-homogenized) TE, TM, and TEM electromagnetic modes supported by the wire medium are orthogonal in each $z=const.$ plane, and thus the tangential component of the electric field associated with each mode must vanish independently at $z=-L$.

The previous discussion implies that the magnetic field given by (4b) can be rewritten as

$$H_y=\left(B_{\mathrm{TEM}}\cos\left((z+L)\beta_h\right)+B_{\mathrm{TM}}\cosh\left((z+L)\gamma_{\mathrm{TM}}\right)\right)$$
$$\times e^{-jk_x x}\quad(\text{wire medium slab}: -L<z<0) \tag{7}$$

where B_{TEM} and B_{TM} are unknown coefficients. Notice that the first term in the right-hand side of the above equation is associated with the TEM mode, whereas the second term is associated with the TM mode. Thus, since the electric field inside the wire medium slab is given by $E_x=-(1/j\omega\varepsilon_0\varepsilon_h)\partial H_y/\partial z$, it is clear that (7) imposes that the x-component of the electric

$$\begin{pmatrix}1 & -\cos(\beta_h L) & -\cosh(\gamma_{\mathrm{TM}}L)\\ -\gamma_0 & \beta_h\varepsilon_h^{-1}\sin(\beta_h L) & -\gamma_{\mathrm{TM}}\varepsilon_h^{-1}\sinh(\gamma_{\mathrm{TM}}L)\\ \gamma_0^2+\beta^2-\beta_h^2 & \beta_h^2\cos(\beta_h L) & -\gamma_{\mathrm{TM}}^2\cosh(\gamma_{\mathrm{TM}}L)\end{pmatrix}\begin{pmatrix}\rho\\ B_{\mathrm{TEM}}\\ B_{\mathrm{TM}}\end{pmatrix}=\begin{pmatrix}-1\\ -\gamma_0\\ -\gamma_0^2-\beta^2+\beta_h^2\end{pmatrix}. \tag{8}$$

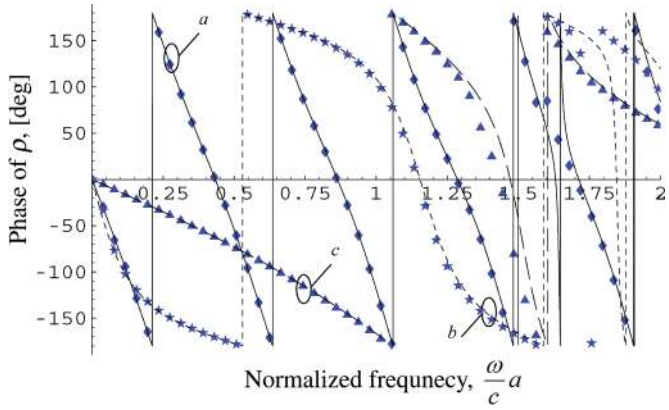

Fig. 2. Phase of the reflection coefficient as a function of the normalized frequency. Solid lines: our analytical model. Discrete symbols: numerical results obtained with a full wave simulator. The permittivity of the dielectric substrate is $\varepsilon_h = 2.2$. The parameters of the problem are: (a) radius of the wires: $r_w = 0.05a$; height of the substrate: $L = 5.0a$; angle of incidence: $\theta = 45°$, (b) $r_w = 0.05a, L = 2.0a, \theta = 80°$, (c) $r_w = 0.01a, L = 1.0a, \theta = 45°$.

field associated with the TEM and TM modes vanish independently at $z = -L$.

Using now the boundary conditions (6), and the proposed field distributions (4a) and (7), we can easily obtain the following definite linear system shown in (8) at the bottom of the previous page. Solving for the reflection coefficient ρ, we obtain the result

$$\rho = \frac{\beta_p^2 \tan(\beta_h L) - k_\parallel^2 \gamma_{\rm TM} \tanh(\gamma_{\rm TM} L) + \varepsilon_h \gamma_0 \left(\beta_p^2 + k_\parallel^2\right)}{\beta_h \beta_p^2 \tan(\beta_h L) - k_\parallel^2 \gamma_{\rm TM} \tanh(\gamma_{\rm TM} L) - \varepsilon_h \gamma_0 \left(\beta_p^2 + k_\parallel^2\right)}. \tag{9}$$

In order to validate the theory, we have numerically calculated the reflection coefficient as a function of frequency using a home made code that implements the method of moments (MoM) (the results were also double-checked using a commercial FDTD electromagnetic simulator). The computed results are depicted in Fig. 2 (discrete symbols) superimposed on the result yielded by our approximate theory (9). As seen, the agreement is very good for a relatively broad range of frequencies even for wide incident angles and relatively short pins. The results of an extensive set of simulations (not reported here for brevity) suggest that the proposed theory is accurate until $\beta_h a$ is comparable with π. This is exactly the scope of validity of the homogenization model (1) for the wire medium. Note that ρ as defined in (4) is the reflection coefficient for the magnetic field (not the electric field) and thus for low frequencies the phase of ρ is zero (rather than 180°). In the next sub-sections, the proposed theory is further validated, and we will discuss the possibility of characterizing the textured surface using an impedance boundary condition.

B. Equivalent Surface Impedance Reactance

In what follows, we study the case where the metallic pins are densely packed, so that the lattice spacing a is extremely small and $L/a \gg 1$. It is shown that only in these conditions the theory of [25] can be applied, and the artificial substrate described by an impedance boundary condition. Moreover, we prove that in these circumstances the effects of spatial dispersion are negligible and that the wire medium can be described using a local permittivity model $\varepsilon_{xx} = \varepsilon_{yy} = \varepsilon_h$ and $\varepsilon_{zz} = \infty$, consistently with the suggestion of [30] to fabricate artificial impedance boundaries. We numerically assess when such simplified impedance reactance model is accurate, and we find that in certain cases it may fail even for moderately small values of the lattice constant, while the general theory proposed in the previous subsection remains valid.

To begin with, we study the limit case in which (for a fixed frequency and thickness L) the spacing between the pins approaches zero, $a \to 0$, and the metal filling fraction is kept constant, or equivalently r_w/a is kept constant. The only parameters in (9) that depend on a or r_w, are β_p and $\gamma_{\rm TM}$. A simple inspection of (2) and of the definition of $\gamma_{\rm TM}$ shows that when $a \to 0$

$$\beta_p \sim \frac{1}{a} \to \infty; \quad \frac{\gamma_{\rm TM}}{\beta_p} \to 1. \tag{10}$$

Thus, using these results in (9), we find that for dense arrays of wires the reflection coefficient is given by

$$\rho \approx -\frac{\beta_h \tan(\beta_h L) + \varepsilon_h \gamma_0}{\beta_h \tan(\beta_h L) - \varepsilon_h \gamma_0}, \quad (k_\parallel \ll \beta_p,\ \beta \ll \beta_p,\ 1 \ll \beta_p L). \tag{11}$$

Quite interestingly, the above formula is exactly the result that one obtains when the effect of the TM-mode in the wire medium slab is neglected, i.e., it is the solution of the scattering problem when the term associated with the coefficient $B_{\rm TM}$ in (7) is discarded (i.e. only the TEM mode is considered), and the classical boundary conditions are enforced at the interface with air. Thus, when the pins are densely packed, the wire medium slab behaves approximately as an anisotropic material with $\varepsilon_{xx} = \varepsilon_{yy} = \varepsilon_h$ and $\varepsilon_{zz} = \infty$ (as described in [27] the TEM mode sees an infinite permittivity along the z direction). Hence, for very densely packed wires the effects of spatial dispersion are negligible. This is understandable because $\gamma_{\rm TM}/\beta$ is very large when the spacing between the wires is small, and thus the TM-mode is strongly attenuated for propagation along z. However, in practical designs the effect of the TM-mode may be important, since it may be difficult to fabricate textured surfaces with the required density of wires. This will be discussed ahead with more detail. It is also interesting to mention that in an array of densely packed wires it is expected that for long wavelengths the specific wire distribution is irrelevant, provided the wires remain aligned along the z-direction, Indeed, the extreme anisotropy of the wire medium is not the result of a resonant phenomenon dependent on the properties of the lattice, but is rather a consequence of the high concentration of wires, more specifically of the fact that $L/a \gg 1$.

Next, we verify that (11) is compatible with the impedance boundary condition proposed in [25]. An ideal isotropic surface impedance is characterized by the following boundary condition [24, p. 233], [30]:

$$\mathbf{E} \times \hat{\boldsymbol{\nu}} = Z_s (\hat{\boldsymbol{\nu}} \times \mathbf{H}) \times \hat{\boldsymbol{\nu}} \tag{12}$$

where Z_s is the surface impedance, and $\hat{\boldsymbol{\nu}}$ is the unit normal vector oriented to the air side ($\hat{\boldsymbol{\nu}} = \hat{\mathbf{u}}_z$ in Fig. 1). The concept of surface impedance is very convenient because it allows

describing in a simplified and intuitive manner the interaction of waves with the artificial substrate. For the geometry understudy, (12) is equivalent to $Z_s = -E_x/H_y$, which evaluated at the air side of the interface yields $Z_s = j\eta_0(\gamma_0/\beta)((\rho-1)/(\rho+1))$ where $\eta_0 = \sqrt{\mu_0/\varepsilon_0}$ is the free-space impedance and ρ is the reflection coefficient for the magnetic field. For densely packed wires, using (11), we find that

$$Z_s = j\eta_0 \frac{1}{\sqrt{\varepsilon_h}} \tan(\beta_h L). \tag{13}$$

This result is completely consistent with the theory of [25] (see also [24, p. 231]), as we wanted to prove. Notice that the expression of Z_s is independent of the angle of incidence due to the effect of the metallic wires. It is important to underline that such remarkable property is only valid for densely packed wires verifying the conditions implicit in the derivation of the formula (11). Otherwise, one needs to consider spatial dispersion effects, and the surface impedance becomes a function of the angle of incidence (or equivalently of $k_{||}$). Hence, our theoretical analysis predicts that, provided one has the means to fabricate very dense arrays of wires so that (10) holds, then there is no physical limit (for PEC wires) on how well the artificial surface may mimic the behavior of an ideal surface impedance given by (13). The effect of metallic losses will be examined in Section III.

The key property of the wire medium that enables the realization of a surface impedance is the fact that the phase velocity (along z) of the TEM mode is independent $k_{||}$ [see (3a)]. This is possible due to the extreme anisotropy of the wire medium, which, under TEM-propagation, effectively behaves as a material with $\varepsilon_{xx} = \varepsilon_{yy} = \varepsilon_h$ and $\varepsilon_{zz} = \infty$, consistently with our previous discussion (a medium with such characteristics was named in [30] a "wave-guiding medium"). In fact, for dense arrays of wires, the metallic wires behave as tiny waveguides whose propagation constant along z is independent of the incidence angle. The value of Z_s at a given frequency can be tuned at will, by controlling the thickness and permittivity of the substrate. It is important to underline that (13) is only valid for TM-polarized incoming waves, since, as referred before, TE-waves do not interact with the metallic pins.

In order to study the possibilities suggested by our theory, next we examine the properties of a surface impedance characterized by $Z_s = j\eta_0$. For simplicity, we consider that the wires stand in air, $\varepsilon_h = 1$. The radius of the wires is $r_w = 0.05a$, where a is the lattice constant. Using (13) it is immediate that the required wire length is $L = \lambda_0/8$ (or equivalently $\beta_h L = \pi/4$), where λ_0 is the free-space wavelength at the design frequency. In Fig. 3 the phase of the reflection coefficient is depicted as a function of the transverse wave vector for different values of a. The solid lines were computed using (9), whereas the discrete symbols were obtained using the MoM. As mentioned before, when $k_{||}/\beta > 1$ the incoming wave is an evanescent plane wave, whereas for $k_{||}/\beta < 1$ we can write $k_{||} = \beta \sin\theta$ where θ is the angle of incidence. The results of Fig. 3 confirm the general good agreement between our theory and the full wave MoM simulations, and demonstrate that the reflection characteristic of the textured surface may depend appreciably on the spacing between the wires. The textured surface is described accurately by the impedance boundary $Z_s = j\eta_0$, only when the

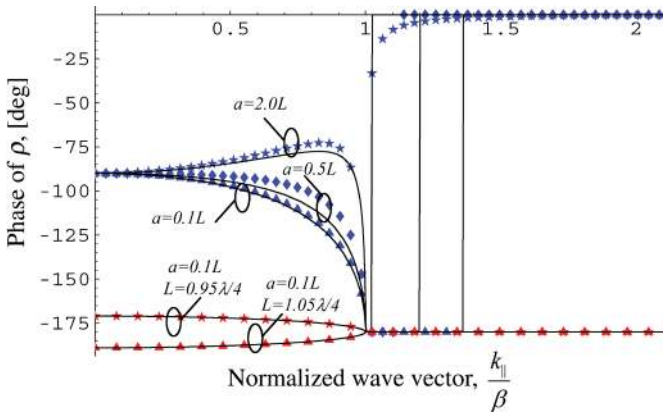

Fig. 3. Phase of the reflection coefficient as a function of the normalized transverse wave vector $k_{||}$, for different values of the lattice constant a. Solid lines: our analytical model. Discrete symbols: numerical results obtained with a full wave simulator. The length of the wires, if not indicated explicitly in the insets, is $L = \lambda_0/8$. The wires stand in air and have radius $r_w = 0.05a$.

wires are closely packed (curve with $a = 0.1L$; this curve is practically coincident with that obtained for an ideal impedance surface $Z_s = j\eta_0$, which, as proved earlier, corresponds to the case $a/L \to 0$ and to the theory of [25]). When the wires are not sufficiently close (roughly for $a/L > 0.3$), the impedance boundary description is not valid and spatial dispersion effects become important. Notice that the phase of the reflection coefficient (in the region $k_{||}/\beta > 1$) changes abruptly from $-180°$ to $0°$. This occurs at the value of $k_{||}$ corresponding to the wave number of the surface wave mode supported by the textured surface.

In a second example, reported also in Fig. 3, we study the possibility of synthesizing an impedance surface that behaves as a perfect magnetic conductor (PMC), $Z_s = \infty$, for TM-polarized waves. As is well-known, the required substrate thickness is $L = \lambda_0/4$ (we still assume that $\varepsilon_h = 1$). In Fig. 3 the reflection characteristic is shown for the cases $L = 1.05\lambda_0/4$ and $L = 0.95\lambda_0/4$, assuming that $a = 0.1L$. It is seen that phase of the reflection coefficient ($\approx -180°$) is nearly independent of the incident angle, even for evanescent waves. This confirms that the textured surface mimics, in fact, the behavior of a PMC ground plane for the considered polarization (as mentioned before, ρ is the reflection coefficient for the magnetic field and so $\rho = -1$ for an ideal PMC ground plane).

It is also interesting to characterize the amplitude of the reflection coefficient. For $k_{||}/\beta < 1$ (propagating incoming wave) it is obvious that conservation of energy requires that $|\rho| = 1$, since all materials are assumed lossless. However, for $k_{||}/\beta > 1$, when the incoming wave is evanescent, the amplitude of the reflection coefficient can have any positive value, and in particular $\rho = \infty$ at the surface wave poles. This is illustrated in Fig. 4 where $|\rho|$ is depicted as a function of normalized $k_{||}$ for the PMC example under study. It is seen that when the wire's length is slightly smaller than $\lambda_0/4$ the reflection coefficient has a pole for a value of $k_{||}/\beta \gg 1$. This indicates that the corresponding surface wave mode is closely bounded to the textured interface. Our analytical theory (9) is able to predict fairly well the behavior of $|\rho|$ for evanescent waves, even though for values of $k_{||}/\beta \gg 1$ the agreement may not be so good. This happens

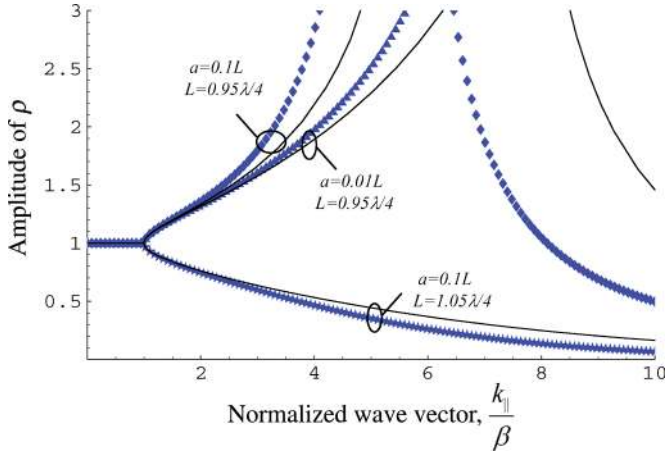

Fig. 4. Amplitude of the reflection coefficient as a function of the normalized transverse wave vector $k_{||}$, for $L = 0.95\lambda_0/4$ or $L = 1.05\lambda_0/4$, $r_w = 0.05a$ and different values of the lattice spacing a. Solid lines: our analytical model. Discrete symbols: numerical results obtained with a full wave simulator. The curve associated with $a = 0.01L$ is practically coincident with the response of an ideal impedance boundary.

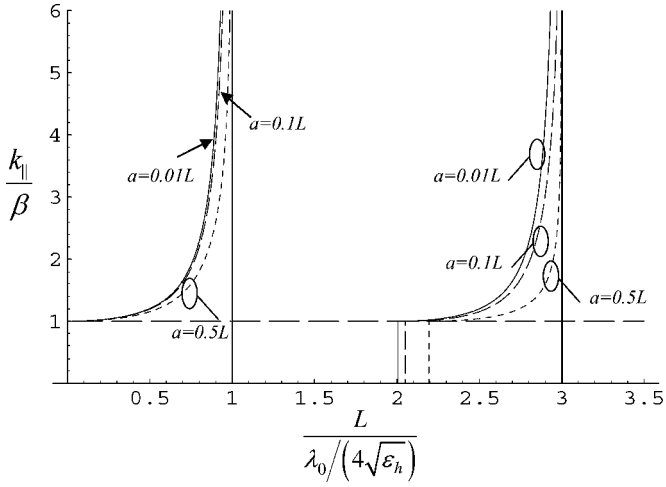

Fig. 5. Normalized wavenumber of the TM-surface wave modes as a function of the normalized thickness of the substrate for different values of the lattice constant. The permittivity of the substrate is $\varepsilon_h = 2.2$ and the radius of the wires is $r_w = 0.05a$.

for two reasons. The first reason is related with the scope of validity of the homogenization model of the wire medium (1), which requires that both $\beta a \ll \pi$ and $k_{||}a \ll \pi$. It is clear that the latter condition may not be fulfilled for large values of $k_{||}$. Consistently with this observation it is seen in Fig. 4 that the agreement between our analytical result and the full wave simulation improves when a/L is decreased from 0.1 down to 0.01. The second reason for the deterioration of agreement is related to the fact that the surface wave pole corresponds to a resonance of the physical system (which is a phenomenon sensitive to small variations of the parameters of the problem), and thus it is not surprising that our approximate model fails to predict exactly the value of $k_{||}$ at the resonance. Nevertheless, (9) is able to describe fairly well the general behavior of $|\rho|$. In particular, it is seen that when the wire length is slightly larger than $\lambda_0/4$, $L = 1.05\lambda_0/4$, the reflection coefficient does not have a pole, and consequently the substrate does not support surface waves. This will be discussed with more detail in the next subsection. Another important result that follows from Fig. 4 is that the properties of surface waves may depend appreciably on the spacing between the wires. In fact, it is seen that when a/L is decreased from 0.1 down to 0.01 the position of the pole varies noticeably, clearly indicating that even when $a/L = 0.1$ the density of wires may not be sufficiently high, and that (11) cannot be used to predict the dispersion characteristic of surface waves (the case $a = 0.01L$ approximates very closely the response of an ideal impedance boundary). This shows that the description of the textured surface as an impedance boundary given by (13) and the theory of [25] may fail even for values of a/L reasonably small, and underlines the importance of the more accurate model (9) proposed in this work.

C. Suppression of TM-Surface Waves

An important application of the microstructured surface under study is the suppression of surface waves in dielectric substrates. In fact, in many antenna problems the excitation of surface waves is not desired, since it may reduce the antenna efficiency and distort the radiation pattern. It is well-known [34, p. 712], that a conventional grounded dielectric substrate supports TM-surface waves for an arbitrary substrate thickness. On the other hand, TE-surface waves may propagate only when $\lambda_0 < \lambda_{co}$, with λ_{co} such that $L = \lambda_{co}/4\sqrt{\varepsilon_h - 1}$.

In what follows, we study the properties of the surface wave modes supported by the "Fakir's bed of nails" substrate. As referred to in Section II-A, since TE-waves do not interact with the metallic pins the dispersion characteristic of the TE-trapped modes is the same as that in the dielectric substrate without the metallic pins (see for example [34, p. 712]). On the other hand, since the poles of ρ correspond to the surface wave modes, the dispersion characteristic of the TM-surface wave modes is obtained by equating the denominator of (9) to zero. Thus, we find that a surface wave mode with wave number $k_{||} = k_{||}(\omega)$ verifies

$$\frac{\beta_h \beta_p^2}{\beta_p^2 + k_{||}^2} \tan(\beta_h L) - \frac{k_{||}^2 \gamma_{\mathrm{TM}}}{\beta_p^2 + k_{||}^2} \tanh(\gamma_{\mathrm{TM}} L) - \varepsilon_h \gamma_0 = 0. \quad (14)$$

Remember that both γ_0 and γ_{TM} are functions of frequency.

We solved numerically the modal equation (14), to obtain $k_{||}$ (wave number of the trapped mode along the interface) as a function of frequency. In Fig. 5 we plot the calculated $k_{||}$ (normalized to the free-space wavenumber) as a function of (the normalized) substrate thickness. As expected, for thin substrates we obtain $k_{||} \approx \beta$ which indicates that the surface wave mode is loosely bound to the textured surface. However, when the substrate thickness is comparable to $\lambda_0/4\sqrt{\varepsilon_h}$ (but still slightly smaller), the wavenumber of the surface wave mode may become large, $k_{||}/\beta \gg 1$, and thus the mode becomes closely attached to the interface. For a substrate thickness slightly larger than $\lambda_0/4\sqrt{\varepsilon_h}$ the propagation of the TM surface wave modes is suppressed. The propagation is resumed for some value of $4L\sqrt{\varepsilon_h}/\lambda_0$ such that $2.0 < 4L\sqrt{\varepsilon_h}/\lambda_0 < 3.0$, and a second stopband occurs when $4L\sqrt{\varepsilon_h}/\lambda_0 \approx 3.0$.

Our theoretical model predicts that the stopband lower frequency is nearly independent of the spacing between the wires

(of course, in order that the theoretical model is meaningful it is always necessary that $\beta_h a \ll \pi$). From Fig. 5 it is seen that when a/L is decreased (keeping r_w/a constant) the value of $k_\parallel/\beta$ increases, and thus the theory suggests that when the wires are densely packed the guided modes become more confined to the surface. On the other hand, the upper frequency of the stopband is notoriously more sensitive to the specific value of a/L. The bandwidth of the stopband is slightly narrower when the wire density is very high. As discussed in Section II-B, very dense arrays of wires may be characterized by the impedance boundary (13). In such circumstances, it is well-known that TM-surface waves propagate when Z_s is inductive, and are suppressed when Z_s is capacitive [15], [23], [24].

To conclude this section, we analyze the possibility of designing a textured surface with a stopband for both TE- and TM-polarizations (i.e., with a complete band gap). Since, as discussed above, TE-modes are cutoff for $\lambda_0 > \lambda_{co}$, it is clear that typically a grounded dielectric substrate with metallic pins has a complete surface wave band gap for the range of wavelengths such that $4L\sqrt{\varepsilon_h - 1} < \lambda_0 < 4L\sqrt{\varepsilon_h}$. The bandwidth of the complete band gap may be narrow when $\varepsilon_h \gg 1$, but may be acceptable for substrates with moderate ε_h.

III. Effect of Metal Losses

In the previous section, the effect of metal losses was neglected and the metals were assumed to be perfect conductors. In general, this is a good approximation at microwaves. In particular, it was shown that a textured surface formed by a densely packed array of PEC pins may mimic almost exactly (apart from technological limitations in the fabrication of the microstructured surface) the behavior of an impedance surface. However, intuitively it is expected that the effect of losses may become increasingly important when the cross-section of the metallic wires is small, i.e., in the limit $a \to 0$ with r_w/a constant. The physical reason is clear: the electric current along a wire with small radius is very large, and thus the effect of losses may become significant. The objective of this section is to discuss in a quantitative manner how losses affect and may limit the performance of the textured surface.

At microwaves, it is a good approximation to consider that metals are described by an electric conductivity σ. The corresponding (relative) permittivity model is

$$\varepsilon_{\text{metal}} = 1 + \frac{\sigma}{j\omega\varepsilon_0} = 1 + \frac{2}{j(\beta\delta_{\text{skin}})^2} \tag{15}$$

where $\delta_{\text{skin}} \approx \sqrt{2/\mu_0\sigma\omega}$ is the skin-depth of the metal, and $\beta = \omega/c$. In our previous work [28], we investigated the properties of a wire medium formed by "non-ideal" metallic rods, with finite conductivity. In particular, we found out that such metamaterial may be described to a good approximation by a dielectric function $\overline{\overline{\varepsilon}}_{\text{eff}}$ defined as in (1), with

$$\varepsilon_{zz}(\omega, k_z) = 1 + \frac{1}{\frac{\varepsilon_h}{(\varepsilon_{\text{metal}} - \varepsilon_h) f_V} - \frac{\beta_h^2 - k_z^2}{\beta_p^2}} \tag{16}$$

where $f_V = \pi(r_w/a)^2$ is the volume fraction of the rods. Note that $\varepsilon_{zz}(\omega, k_z)$ defined as in (1) is the particular case of the above formula when the wires are PEC, i.e., when $\varepsilon_{\text{metal}} = -\infty$. As discussed in [7], [28] when the rods have finite conductivity the wire medium supports a quasi-TEM mode. The dispersion characteristic of the quasi-TEM mode can be written in the general form $k_{z,\text{TEM}} = k_{z,\text{TEM}}(\omega, k_\parallel)$ (see [7], [28] for the detailed expression). As proven in Section II-B, for very densely packed arrays of wires the effect of the TM mode can be neglected, and the properties of the textured surface can be predicted using only the quasi-TEM mode and classical boundary conditions. Straightforward calculations show that in these conditions the reflection coefficient is to a first approximation [(compare with (11)]

$$\rho \approx -\frac{k_{z,\text{TEM}} \tan(k_{z,\text{TEM}} L) + \gamma_0 \varepsilon_h}{k_{z,\text{TEM}} \tan(k_{z,\text{TEM}} L) - \gamma_0 \varepsilon_h} \qquad (k_\parallel \ll \beta_p,\ \beta \ll \beta_p, 1 \ll \beta_p L). \tag{17}$$

Following [7], [28], we have that

$$k_{z,\text{TEM}}^{(0)} = k_{z,\text{TEM}}|_{k_\parallel = 0} \approx \beta_h \tag{18a}$$

$$k_{z,\text{TEM}}^{(\infty)} = k_{z,\text{TEM}}|_{k_\parallel = \infty} = \sqrt{\beta_h^2 + \beta_c^2},$$

$$\beta_c^2 = -\frac{\varepsilon_h \beta_p^2}{(\varepsilon_{\text{metal}} - \varepsilon_h) f_V}. \tag{18b}$$

Thus, unlike the case of PEC rods (for which β_c defined as above vanishes) the quasi-TEM is not dispersionless, i.e., $k_{z,\text{TEM}}(\omega, k_\parallel)$ is not independent of $k_\parallel$, or in other words the phase velocity along z depends on the transverse phase shift $k_\parallel$. It is evident that the textured surface is equivalent to a surface impedance only when the dependence of $k_{z,\text{TEM}}(\omega, k_\parallel)$ on $k_\parallel$ can be neglected. Thus the parameter $k_{z,\text{TEM}}^{(\infty)}/k_{z,\text{TEM}}^{(0)}$ can be used to assess the effect of the finite conductivity of the rods. If $k_{z,\text{TEM}}^{(\infty)}/k_{z,\text{TEM}}^{(0)}$ is close to unity the effect of losses may be considered negligible, otherwise it may completely modify the properties of the textured surface.

Using (15) and (18) we obtain after straightforward calculations (it is assumed that ε_h is not very different from unity) that

$$\frac{k_{z,\text{TEM}}^{(\infty)}}{k_{z,\text{TEM}}^{(0)}} \approx \sqrt{1 - \frac{j}{2\pi}(\beta_p a)^2 \left(\frac{\delta_{\text{skin}}}{r_w}\right)^2}. \tag{19}$$

For typical designs $\beta_p a$ given by (2) is in the range $1.0 < \beta_p a < 2.5$ (this parameter cannot be made too small because the plasma frequency varies with the logarithm of r_w/a). Thus, (19) demonstrates that $k_{z,\text{TEM}}^{(\infty)}/k_{z,\text{TEM}}^{(0)}$ can be close to unity if and only if $\delta_{\text{skin}}/r_w \ll 1$, i.e., the effect of metallic losses is negligible provided the skin depth of the metal is significantly smaller than the radius of the wires.

To give an idea of the suggested possibilities, let us consider that the rods are made of copper with $\sigma = 5.8 \times 10^7\ \text{S/m}$ around $\lambda_0 = 3\ \text{cm}$. The corresponding metal skin depth is such that $\delta_{\text{skin}}/\lambda_0 \approx 3.8 \times 10^{-5}/\sqrt{\lambda_{0,\text{cm}}}$, where the subscript "cm" indicates that $\lambda_{0,\text{cm}}$ is specified in centimeters. Choosing the critical value $r_w \approx 10\delta_{\text{skin}}$ and assuming that $r_w/a = 0.1$, we conclude that the minimum spacing between the metallic wires that may still allow neglecting losses is such that $a_{min}/\lambda_0 \approx 3.8 \times 10^{-3}/\sqrt{\lambda_{0,\text{cm}}}$ around $\lambda_0 = 3\ \text{cm}$. Thus, this result suggests that at centimeter waves the effect of losses may be neglected even for arrays of wires with a/λ_0 as small as 10^{-3},

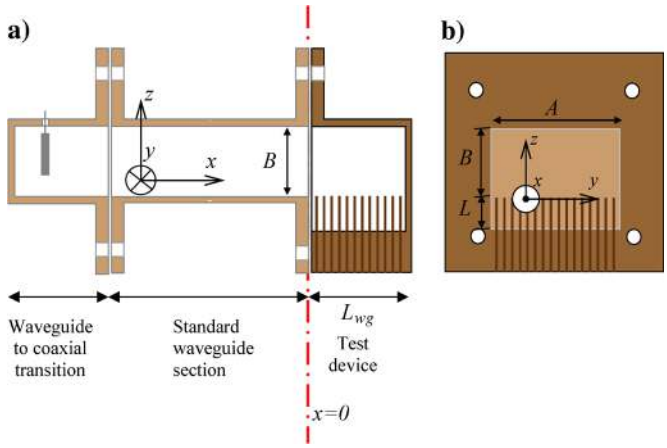

Fig. 6. Geometry of the experimental setup: a standard X-band rectangular waveguide fed by a coaxial probe is loaded with a test device. One of the walls of the test device is perforated with metallic pins. (a) E-plane cut. (b) H-plane cut.

and thus we conclude that apart from technological limitations it is possible in fact to synthesize artificial textured surfaces that follow almost exactly (13).

IV. Experimental Validation

In the previous sections, we studied the properties of the "Fakir's bed of nails" substrate, assuming always that the substrate is unbounded and periodic along the x and y directions. However, in a realistic setup the textured surface has necessarily finite dimensions and a finite number of pins. In the following, the objective is to examine the properties of a finite sized textured surface, and verify if it may still be characterized using the proposed analytical models. The idea is to test the response of the "Fakir's bed of nails" substrate in a closed metallic waveguide environment, as illustrated in Fig. 6. The setup consists of a standard X-band metallic waveguide with rectangular cross-section $A \times B$ connected to a second waveguide (test device) in which one of the walls is a textured surface corrugated with metallic pins of height L. The test device has length L_{wg} and is terminated in short-circuit. The test device is illuminated with the fundamental TE_{10} mode.

To begin with, we characterize some basic properties of the waveguide modes supported by the test device. The structure under study may be regarded as a metallic waveguide partially filled with a wire medium slab ($-L < z < 0$ and $0 < y < A$) and partially filled with air ($0 < z < B$ and $0 < y < A$). Note that the metallic pins are oriented along the z-direction, and that the direction propagation in the metallic waveguide is along x. It is well known that the normal modes of propagation in partially filled waveguides are not, in general, either TE or TM modes [34]. Instead the modes can be classified as longitudinal-section electric (LSE) and longitudinal-section magnetic (LSM) modes [34]. In our notations, the LSE modes are such that $E_z = 0$ (derives from a magnetic-type Hertzian potential directed along z), and the LSM modes are such that $H_z = 0$ (derives from an electric-type Hertzian potential directed along z). It is not our objective to present an exhaustive study of the properties of the normal modes of propagation. We are mainly interested in the properties of the fundamental waveguide mode, which is an LSM mode. In Appendix A, we derive the field distributions and modal equation of the LSM modes. The main result, (A6), relates the propagation constant of the waveguide modes, $k_x = k_{x,wg}(\omega)$, with the geometrical parameters of the structure and with frequency. In case the metallic pins are densely packed so that the interface $z = 0$ can be regarded as an impedance surface, the modal equation is given by (A7).

When the fundamental TE mode (that propagates in the standard waveguide section; see Fig. 6) impinges on the device under test, it will excite many waveguide modes. In fact, (A2) and (A3) show that the transverse electromagnetic field distribution of the standard TE mode is different from the field distribution of the LSM modes supported by the device under test. Thus, rigorously speaking, an infinite numerable set of modes may be excited to enforce the mode matching at the interface. Nevertheless, for relatively low frequencies, it may be a good approximation to consider that only the fundamental LSM mode is excited, and that the effect of higher order modes is negligible. We will use this approximation to obtain an estimate of the reflection coefficient R_{wg} at the interface. Since the metallic waveguide is terminated by a short-circuit wall (placed at $x = L_{wg}$), it is straightforward to verify that the reflection coefficient for the electric field R_{wg} at the input plane ($x = 0$) is given by

$$R_{wg} = \frac{\eta_{wg} j \tan(k_{x,wg} L_{wg}) - \eta_{\mathrm{TE10}}}{\eta_{wg} j \tan(k_{x,wg} L_{wg}) + \eta_{\mathrm{TE10}}}$$
$$\eta_{wg} = \eta_0 \frac{\left(\frac{\pi}{A}\right)^2 + k_{x,wg}^2}{\beta k_{x,wg}} \tag{20}$$

where $\eta_{\mathrm{TE10}} = \eta_0 \beta / \sqrt{\beta^2 - (\pi/A)^2}$ is the transverse impedance of the TE mode, $k_{x,wg}$ is the propagation constant of the fundamental LSM mode (obtained from the numerical solution of (A6) with respect to k_x and using $n = 1$), and η_{wg} is the transverse impedance of the fundamental LSM mode.

In order to test the proposed theory, we fabricated a Fakir's bed substrate formed by an array of 9×20 pins standing in air ($\varepsilon_h = 1$). The cross-section of the metallic waveguide is $A \times B = 22.8\ \mathrm{mm} \times 10\ \mathrm{mm}$. The number of pins in the transverse y-direction is 9 and along the x-direction the number is 20. The waveguide walls are $a/2$ away from the adjacent row of pins. Thus, the spacing between the metallic pins is $a = A/9 = 2.53\ \mathrm{mm}$ and the length of the device under test is $L_{wg} = 20a = 50.67\ \mathrm{mm}$. The height of the metallic pins is $L = 3.75\ \mathrm{mm}$ and its diameter is $2r_w = 2 \times 0.09a = 0.47\ \mathrm{mm}$. A photo of the fabricated prototype is shown in Fig. 7.

In Fig. 8 we depict the phase of the s11-parameter measured using the Agilet 8361A vector network analyzer (curve a), superimposed on the result obtained with our analytical model (20), using equation (A6) to obtain $k_x = k_{x,wg}(\omega)$ (curve b). It is seen that despite the several approximations that were made, the two curves are nearly coincident through the whole X-band 8-12GHz, apart from some fluctuations mainly resulting from imperfections of the experimental setup. This further validates our theory, and confirms that it may be useful and accurate even when the textured surface has finite dimensions. In this configuration, the effect of the textured surface on the wave propagation

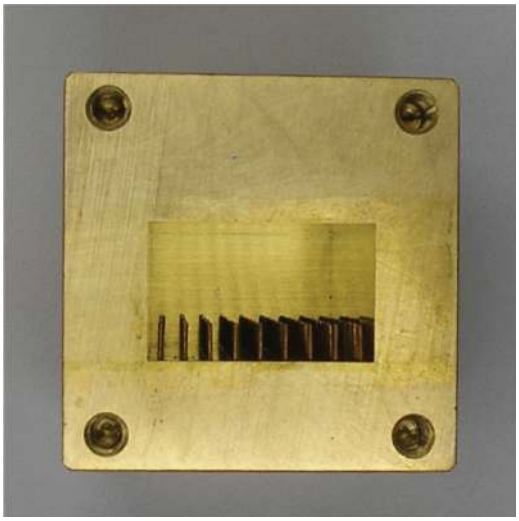

Fig. 7. Photo of the fabricated prototype.

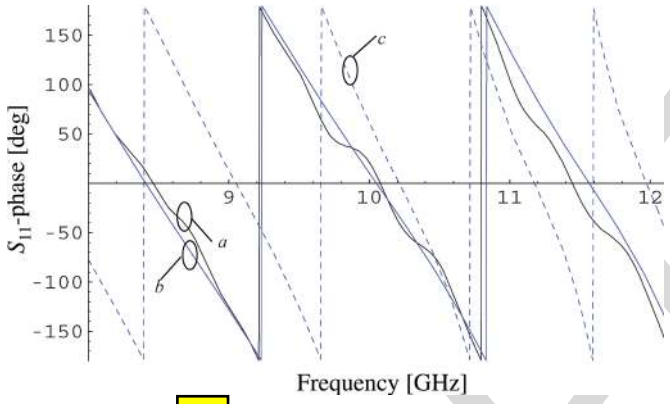

Fig. 8. Phase of the S_{11} parameter as a function of frequency. (a) Experimental result obtained with a vector network analyzer. (b) Analytical model taking into account the effects of spatial dispersion [see (20) and (A6)]. (c) Analytical model assuming that the textured substrate is equivalent to a surface impedance [see (20) and (A7)].

is to some extent equivalent to that of filling the waveguide with a dielectric material. Indeed, in the frequency interval 8-12GHz, $k_{x,wg}$ is such that $0.83 < k_{x,wg}/\beta < 1.19$ (inside the test device). If a PEC wall is placed at $z = 0$ one would obtain instead $0.57 < k_{x,wg}/\beta < 0.84$.

It is also worth noting that for this example, the approximation that describes the textured surface as an impedance boundary is too coarse to yield accurate results (curve c in Fig. 8). In fact, the fabricated prototype has $a/L = 0.67$, and thus the density of pins is insufficient to make (13) accurate. This further underlines that only densely packed wires are accurately described by the theory of [25], and that otherwise spatial dispersion effects need to be considered.

V. Conclusion

In this work, it was proved that a textured surface formed by metallic wires connected to a ground plane can be accurately characterized using homogenization techniques. It was shown that the textured surface is equivalent to a wire medium slab, and that its reflection properties and guided mode characteristics may be accurately predicted by taking into account spatial dispersion effects. Our results demonstrate that nonlocal effects may be neglected only if the wires are very densely packed ($L/a \gg 1$). A key result of this paper establishes that it may be possible to create a textured surface that behaves exactly as an ideal impedance surface (for TM-polarization), provided one has the ability to fabricate a substrate with densely packed metallic wires. The value of the surface reactance can be tuned at will by varying the thickness or the dielectric constant of the substrate. Furthermore, we have shown that in principle the effect of metallic losses may be neglected at microwaves, even for wires with very thin radius. Finally, we presented experimental data that further validates the proposed analytical models, even in a waveguide configuration where the textured surface has finite-size and a finite number of pins. The considered substrates may have interesting applications in the design of surface impedances, and may in principle be fabricated using standard printed circuit techniques (by drilling holes in a dielectric substrate that are afterwards plated with copper), or alternatively using low temperature co-fired ceramic (LTCC) technology.

Appendix A

In this Appendix, we derive the modal equation for the LSM modes supported by a waveguide partially filled with wire medium (test device in Fig. 6). The simplest way to obtain the field distribution of the LSM modes is to use the results of Section II-A, where we studied the reflection of plane waves by a Fakir's bed of nails substrate standing in free-space. In particular, the results of Section II-A imply that in the air region, $z > 0$, the following family of electromagnetic modes satisfies Maxwell's Equations:

$$\mathbf{H} \propto \mathbf{k}_{||} \times \hat{\mathbf{u}}_z g(z,k_{||}) e^{-j\mathbf{k}_{||}\cdot\mathbf{r}} = (k_y, -k_x, 0) g(z,k_{||}) e^{-j\mathbf{k}_{||}\cdot\mathbf{r}} \quad z>0 \tag{A1a}$$

$$g(z,k_{||}) = e^{+\gamma_0 z} + \rho e^{-\gamma_0 z} \tag{A1b}$$

where $\mathbf{k}_{||} = (k_x, k_y, 0)$, $\gamma_0 = \sqrt{k_{||}^2 - \beta^2}$, and ρ is given by (9). We underline that the magnetic field distribution given by (A1) satisfies the Maxwell-equations in the air region for arbitrary $\mathbf{k}_{||}$, and in addition satisfies the proper boundary conditions at the textured surface at $z = 0$. Next, the idea is to judiciously combine solutions of the form (A1), in order to obtain waveguide modes that also satisfy the correct boundary conditions at the metallic walls $y = 0$, $y = A$, and $z = B$ (see Fig. 6). More specifically, an anti-symmetric linear combination of solutions with wave vectors $(k_x, k_y, 0)$ and $(k_x, -k_y, 0)$ yields the following generic family of solutions

$$\mathbf{H} = H_0 \left(\frac{k_y}{\beta} \cos(k_y y), \frac{jk_x}{\beta} \sin(k_y y), 0 \right) g(z,k_{||}) e^{-jk_x x},\ z>0 \tag{A2}$$

where H_0 is an arbitrary constant that defines the amplitude of the magnetic field. The corresponding electric field $\mathbf{E} = \nabla \times \mathbf{H}/j\omega\varepsilon_0$ is

$$\mathbf{E} = \frac{\eta_0 H_0}{j\beta} \left(-\frac{jk_x}{\beta} \sin(k_y y) \frac{dg}{dz}, \frac{k_y}{\beta} \cos(k_y y) \frac{dg}{dz}, \right.$$

$$\left.\frac{k_{\|}^2}{\beta}\sin(k_y y)g\right) e^{-jk_x x}. \quad \text{(A3)}$$

In order that the tangential electric field vanishes at the PEC walls $y=0$, $y=A$, and $z=B$, it is necessary that

$$\sin(k_y A)=0; \quad \left.\frac{dg}{dz}\right|_{z=B}=0 \quad \text{(A4)}$$

Hence, using (A1b), we conclude that the LSM modes are characterized by $k_y = n\pi/A$, $n=1,2,3,\ldots$, and have propagation constant k_x such that

$$e^{+\gamma_{0,n}B}-\rho e^{-\gamma_{0,n}B}=0, \quad \gamma_{0,n}=\sqrt{\left(\frac{n\pi}{A}\right)^2+k_x^2-\beta^2} \quad \text{(A5)}$$

where ρ is given by (9). Simplifying the above equation we obtain the following modal equation for the LSM modes:

$$\frac{\beta_h\beta_p^2}{\beta_p^2+k_{\|,n}^2}\tan(\beta_h L)-\frac{k_{\|,n}^2\gamma_{\mathrm{TM,n}}}{\beta_p^2+k_{\|,n}^2}\tanh(\gamma_{\mathrm{TM},n}L)- \varepsilon_h\gamma_0\tanh(\gamma_{0,n}B)=0 \quad \text{(A6)}$$

where $\gamma_{\mathrm{TM},n}=\sqrt{\beta_p^2+(n\pi/A)^2+k_x^2-\beta_h^2}$ and $k_{\|,n}=\sqrt{(n\pi/A)^2+k_x^2}$. Note that when the height of the pins is zero, $L=0$, the modal equation is equivalent to $\tanh(\gamma_{0,n}B)=0$, which gives the classical formula for the propagation constant in a metallic waveguide with rectangular cross-section $k_x=\sqrt{\beta^2-(n\pi/A)^2-(m\pi/B)^2}$, with n and m integers. In case the metallic pins are densely packed so that formula (10) is valid and the textured surface is equivalent to the surface impedance (13), the modal equation simplifies to

$$\beta_h\tan(\beta_h L)-\varepsilon_h\gamma_0\tanh(\gamma_{0,n}B)=0. \quad \text{(A7)}$$

ACKNOWLEDGMENT

The authors thank V. Fred for his technical assistance in the fabrication of the textured surface prototype.

REFERENCES

[1] F. Falcone, T. Lopetegi, J. D. Baena, R. Marqués, F. Martín, and M. Sorolla, "Effective negative- ε stop-band microstrip lines based on complementary split ring resonators," *IEEE Microw. Wireless Compon. Lett.*, vol. 14, pp. 280–282, Jun. 2004.

[2] N. Engheta, "An idea for thin, subwavelength cavity resonators using metamaterials with negative permittivity and permeability," *IEEE Microw. Wireless Compon. Lett.*, vol. 1, p. 10, 2002.

[3] A. Alù and N. Engheta, "Pairing an epsilon-negative slab with a mu-negative slab: Resonance, tunneling, and transparency," *IEEE Trans. Antennas Propag.*, vol. 51, p. 2558, 2003.

[4] A. Grbic and G. V. Eleftheriades, "Overcoming the diffraction limit with a planar left handed transmission line lens," *Phys. Rev. Lett.*, vol. 92, p. 117403, Mar. 2004.

[5] C. Luo, S. G. Johnson, J. D. Joannopoulos, and J. Pendry, "Subwavelength imaging in photonic crystals," *Phys. Rev. B*, vol. 68, 2[illegible] 045115(1-15).

[6] P. A. Belov, Y. Hao, and S. Sudhakaran, "Subwavelength microwave imaging using an array of parallel conducting wires as a lens," *Phys. Rev. B*, vol. 73, 2006, 033108([illegible]

[7] M. Silveirinha, P. A. Belov, and C. Simovski, "Subwavelength imaging at infrared frequencies using [illegible]rray of metallic nanorods," *Phys. Rev. B*, vol. 75, 2007, 035108([illegible]

[8] M. Silveirinha and N. Engheta, "Tunneling of electromagnetic energy through sub-wavelength channels and bends [illegible] near-zero-epsilon materials," *Phys. Rev. Letts.*, vol. 97, 2006, 15[illegible]

[9] A. S. Ilyinski, G. Y. Slepyan, and A. Y. Slepyan, "Propagation, scattering and dissipation of electromagnetic waves," IEE Electromagnetic Waves Series 36. London, U.K., 1993, ch. 5.

[10] W. Rotman, "A study of single-surface corrugated guides," *Proc. IRE*, vol. 39, pp. 952–959, Aug. 1951.

[11] R. Elliot, "On the theory of corrugated plane surfaces," *IRE Trans. Antennas Propag.*, vol. 2, pp. 71–81, Apr. 1954.

[12] S. Lee and W. Jones, "Surface waves on two-dimensional corrugated surfaces," *Radio Sci.*, vol. 6, pp. 811–818, 1971.

[13] S. A. Maier, S. R. Andrews, L. Martín-Moreno, and F. J. García-Vidal, "Terahertz surface plasmon-polariton propagation and focusing o[illegible] riodically corrugated metal wires," *Phys. Rev. Letts.*, vol. 97, [illegible] 176805.

[14] D. Sievenpiper, "High-impedance electromagnetic surfaces," Ph.D. dissertation, Dept. Elect. Eng., UCLA, Los Angeles, CA, 1999.

[15] D. Sievenpiper, L. Zhang, R. Broas, N. Alexopolous, and E. Yablonovitch, "High-impedance electromagnetic surfaces with a forbidden frequency band," *IEEE Trans. Microw. Theory Tech.*, vol. 47, pp. 2059–2074, Nov. 1999.

[16] H. Y. Yang, R. Kim, and D. R. Jackson, "Design consideration for modeless integrated circuit substrates using planar periodic patches," *IEEE Trans. Microw. Theory Tech.*, vol. 48, p. 2233, Dec. 2000.

[17] R. F. Jimenez Broas, D. F. Sievenpiper, and E. Yablonovitch, "A high-impedance ground plane applied to a cellphone handset geometry," *IEEE Trans. Microw. Theory Tech.*, vol. 49, pp. 1262–1265, July 2001.

[18] F. Yang and Y. Rahmat-Samii, "Reflection phase characterizations of the EBG ground plane for low profile wire antenna applications," *IEEE Trans. Antennas Propag.*, vol. 51, pp. 2691–2703, Oct. 2003.

[19] F. Yang, A. Aminian, and Y. Rahmat-Samii, "A novel surface wave antenna design using a thin periodically loaded ground plane," *Microw. Opt. Technol. Lett.*, vol. 47, pp. 240–245, Nov. 2005.

[20] H. Mosallaei and K. Sarabandi, "Antenna miniaturization and bandwidth enhancement using a reactive impedance substrate," *IEEE Trans. Antennas Propag.*, vol. 52, pp. 2403–2414, 2004.

[21] A. P. Feresidis, G. Goussetis, S. Wang, and J. C. Vardaxoglou, "Artificial magnetic conductor surfaces and their application to low-profile high-gain planar antennas," *IEEE Trans. Antennas Propag.*, vol. 53, pp. 209–215, 2005.

[22] S. Tretyakov and C. Simovski, "Dynamic model of artificial reactive impedance surfaces," *J. Electromagn. Waves Applicat.*, vol. 17, pp. 131–145, 2003.

[23] N. Engheta and R. W. Ziolkowski, Eds., *Metamaterials—Physics and Engineering Explorations*. New York: Wiley, 2006, ch. 11 and 12.

[24] S. A. Tretyakov, *Analytical Modeling in Applied Electromagnetics*. Norwood, MA: Artech House, 2003, ch. 6.

[25] R. J. King, D. V. Thiel, and K. S. Park, "The synthesis of surface reactance using an artificial dielectric," *IEEE Trans. Antennas Propag.*, vol. 31, no. 3, p. 471, May 1983.

[26] S. Clavijo, R. E. Díaz, and W. E. McKinzie, III, "Design methodology for sievenpiper high-impedance surfaces: An artificial magnetic conductor for positive gain electrically small antennas," *IEEE Trans. Antennas Propag.*, vol. 51, no. 10, pp. 2678–2690, Oct. 2003.

[27] P. A. Belov, R. Marques, S. I. Maslovski, I. S. Nefedov, M. Silveirinha, C. R. Simovski, and S. A. Tretyakov, "Strong spatial dispersion in wire me[illegible]he very large wavelength limit," *Phys. Rev. B*, vol. 67, 2003, 113[illegible]

[28] M. Silveirinha, "Nonlocal homogenization model for a per[illegible]rray of epsilon-negative rods," *Phys. Rev. E*, vol. 73, 2006, 0466[illegible]0).

[29] M. Silveirinha and C. A. Fernandes, "Homogenization of 3D-connected and non-connected wire metamaterials," *IEEE Trans. Microw. Theory Tech.*, vol. 53, no. 4, pp. 1418–1430, Apr. 2005, Special Issue on Metamaterials.

[30] I. V. Lindell and A. H. Sihvola, "Realization of impedance boundary," *IEEE Trans. Antennas Propag.*, vol. 54, pp. 3669–3676, 2006.

[31] M. Silveirinha, "Additional boundary condition for the wire medium," *IEEE Trans. Antennas. Propag.*, vol. 54, p. 1766, 2006.

[32] V. Agranovich and V. Ginzburg, *Spatial Dispersion in Crystal Optics and the Theory of Excitons*. New York: Wiley-Interscience, 1966.

[33] P. A. Belov and M. Silveirinha, "Resolution of subwavelength transmission devices formed by a wire medium," *Phys. Rev. E*, vol. 73, 2006, 0566[illegible]).

[34] R. E. Collin, *Field Theory of Guided Waves*, 2nd ed. New York: IEEE Press, 1991, pp. 411–416.

Mário G. Silveirinha (S'99–M'03) received the "Licenciado" degree in electrical engineering from the University of Coimbra, Portugal, in 1998 and the Ph.D. degree in electrical and computer engineering from the Instituto Superior Técnico (IST), Technical University of Lisbon, Lisbon, Portugal, in 2003.

Since 2003, he has been an Assistant Professor at the University of Coimbra. His research interests include electromagnetic wave propagation in structured materials and homogenization theory.

Carlos A. Fernandes (**AUTHOR: PLEASE PROVIDE THE LAST TWO DIGITS OF IEEE MEMBERSHIP YEAR**) received the Licenciado, M.Sc., and Ph.D. degrees in electrical and computer engineering from the Instituto Superior Técnico (IST), Technical University of Lisbon, Lisbon, Portugal, in 1980, 1985, and 1990, respectively.

In 1980, he joined the Department of Electrical and Computer Engineering, IST, where he is presently a Full Professor In the areas of microwaves, radio wave propagation and antennas. He is also a Senior Researcher at the Instituto de Telecomunicações, where he is the Coordinator of the Wireless Communications scientific area. He has been the leader of antenna activity in National and European Projects such as RACE 2067—MBS (Mobile Broadband System), ACTS AC230—SAMBA (System for Advanced Mobile Broadband Applications) and ESA/ESTEC—ILASH (Integrated Lens Antenna Shaping). He has coauthored a book, a book chapter, and several technical papers in international journals and conference proceedings, in the areas of antennas and radiowave propagation modeling. His current research interests include artificial dielectrics, dielectric antennas for millimeter wave applications, and propagation modeling for mobile communication systems.

Jorge R. Costa (S'97–M'03) was born in Lisbon, Portugal, in 1974. He received the Licenciado and Ph.D. degrees in electrical engineering from the Instituto Superior Técnico, Lisbon, Portugal, in 1997 and 2002, respectively.

He is currently a Researcher at the Instituto de Telecomunicações, Lisbon. He is also an Assistant Professor at the Departamento de Ciência e Tecnologias da Informação, Instituto Superior das Ciências do Trabalho e da Empresa. His present research interests include lenses, reconfigurable antennas, MEMS switches, and RFID antennas.